

Sensor Motion Tracking by IMM-Based Extended Kalman Filters

Chin-Der Wann and Jian-Hau Gao

Department of Electrical Engineering

National Sun Yat-Sen University

70, Lien-Hai Road, Kaohsiung, 80424, Taiwan

E-mail: cdwann@mail.nsysu.edu.tw

Abstract—In this paper, we present a real-time motion estimation and tracking scheme using interacting multiple model (IMM) based Kalman filters. In the proposed IMM-based structure, two filters, quaternion-based extended Kalman filter (QBEKF) and gyroscope-based extended Kalman filter (GBEKF) are utilized for sensor motion state estimation. In the QBEKF, measurements from gyroscope, accelerometer and magnetometer are processed; while in the GBEKF, sole measurements from gyroscope are processed. The interacting multiple model algorithm is capable of adaptively fusing the estimated states from the two models, and generating better estimation results via the flexibility of model weighting. Simulation results validate the proposed estimator design concept, and show that the scheme is capable of reducing the overall estimation errors.

Index Terms—Motion Tracking; interacting multiple model; extended Kalman filter; motion estimation;

I. INTRODUCTION

In recent years, applications of micro-electro-mechanical systems based inertial sensors in human body motion estimation have attracted significant amount of attention in academia, research and industry. Accurate orientation estimation in human body motion has a widespread use in virtual reality, robotics, and biomedical applications [1]. Motion sensors such as gyroscope, accelerometer and magnetometer are used to determine location by measuring physical parameters, for instance, position, acceleration and angular velocity, which are directly related to the motions of desired targets or the body parts where sensors are placed. The gyroscope can be used to determine orientation, however, only for relatively short period of time since the bias of gyroscope would tend to drift over time. This orientation needs to be continuously corrected by using additional complementary sensors [2].

Extended Kalman filters have been studied widely for real-time estimation of parameters. The filter can also process data from small inertial/magnetic sensor modules containing triaxial angular rate sensors, accelerometers, and magnetometers [2], [3]. In representing the finite rotation parameters, quaternion are used due to the capacity in specifying arbitrary rotations in space without degeneration to singularity [4]. To integrate estimates from different estimation models, a scheme with the interacting multiple model (IMM) algorithm [5], [6] is proposed.

The paper is organized as follows. Section II describes sensor signal models and the quaternion representation.

The designs and implementations of quaternion-based extended Kalman filter (QBEKF) and gyroscope-based extended Kalman filter (GBEKF) are presented. Section III describes the IMM-based structure with the two EKF models. Section IV provides simulation results and discussions. Finally, the conclusions are given in Section V.

II. SENSOR SIGNAL MODEL

In sensor systems where gyroscope, accelerometer, and magnetometer are used, the three-dimensional state vectors in X , Y and Z axes can be transformed and represented as

$$\boldsymbol{\omega} = \boldsymbol{\omega}_{true} + \boldsymbol{\omega}_{bias} + \mathbf{n}_{\omega}, \quad (1)$$

$$\mathbf{a} = \mathbf{a}_{true} + \mathbf{n}_a, \quad (2)$$

$$\mathbf{m} = \mathbf{m}_{true} + \mathbf{n}_m, \quad (3)$$

where $\boldsymbol{\omega}$, \mathbf{a} and \mathbf{m} are measurements of gyroscope, accelerometer and magnetometer, respectively; $\boldsymbol{\omega}_{true}$, \mathbf{a}_{true} and \mathbf{m}_{true} are the true values. The \mathbf{n}_{ω} , \mathbf{n}_a and \mathbf{n}_m are assumed zero mean additive White Gaussian noise (AWGN), with standard deviations σ_{ω} , σ_a and σ_m , respectively. The term $\boldsymbol{\omega}_{bias}$ is the gyroscope bias, which generally affects the accuracy of the sensor system and must be accounted for by filtering methods [3]. For three-dimensional motion tracking, a gyroscope can usually be used as the major source of measurements; while the accelerometer and magnetometer are used as supplementary sensors [3], [7].

To perform motion tracking by using supplementary measures from accelerometer and magnetometer, Gauss-Newton algorithm can be used in obtaining the quaternions \mathbf{q} , which are then used in computation of object rotation:

$$\dot{\mathbf{q}} = \frac{1}{2} \mathbf{q} \otimes \boldsymbol{\omega}. \quad (4)$$

After normalization, the estimated quaternion (4) becomes

$$\hat{\mathbf{q}} = \frac{\dot{\mathbf{q}}}{|\dot{\mathbf{q}}|}. \quad (5)$$

The quaternion is a four-dimensional extension to complex numbers. Any quaternion vector belongs to \mathbb{R}^4 space. A quaternion \mathbf{q} can be represented as [4]

$$\mathbf{q} = q_0 + q_1\mathbf{i} + q_2\mathbf{j} + q_3\mathbf{k}, \quad (6)$$

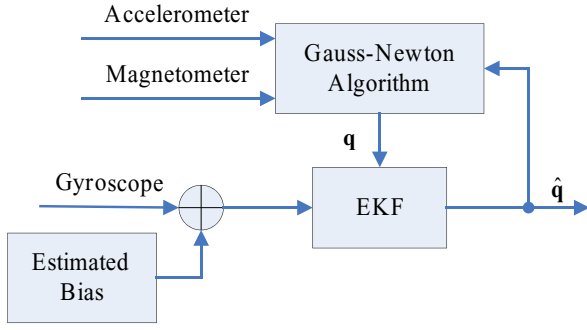


Fig. 1. Block diagram of the QBKF.

or be written as

$$\mathbf{q} = [q_0 \ q_1 \ q_2 \ q_3]^T = [q_0 \ \mathbf{v}]^T \quad (7)$$

where q_0 , q_1 , q_2 and q_3 are real numbers, \mathbf{v} is the vector part (non-scalar part) of quaternion vector, and q_0 is its scalar part in \mathbf{q} . A quaternion vector satisfies a single constraint given by $\mathbf{q}^T \mathbf{q} = 1$. Detail of the computation with quaternion can be found in [4].

To represent the rotating angle with quaternion, (7) can be rewritten as

$$\mathbf{q} = \left[\cos\left(\frac{\theta}{2}\right) \ \mathbf{u} \sin\left(\frac{\theta}{2}\right) \right] \quad (8)$$

where θ is the rotating angle, and \mathbf{u} is a three-dimensional rotating vector. Based on (7), the multiplication of two quaternions \mathbf{q}_1 and \mathbf{q}_2 can be defined as

$$\mathbf{q}_1 \otimes \mathbf{q}_2 = \begin{bmatrix} q_{10}q_{20} - \mathbf{v}_1 \cdot \mathbf{v}_2 \\ q_{10}\mathbf{v}_2 + q_{20}\mathbf{v}_1 + \mathbf{v}_1 \times \mathbf{v}_2 \end{bmatrix} \quad (9)$$

where q_{10} and q_{20} are the scalar term q_0 in \mathbf{q}_1 and \mathbf{q}_2 , respectively. The operator ‘ \cdot ’ denotes an inner product, while ‘ \times ’ denotes an outer product. The rotation angle θ of vector \mathbf{p} , if represented by quaternion, can be written as

$$\mathbf{p}_{rotated} = \mathbf{q}^{-1} \mathbf{p} \mathbf{q}. \quad (10)$$

III. IMM-BASED EXTENDED KALMAN FILTERS

A. Quaternion/Gyroscopic-based EKFs

Extended Kalman filters have been widely used in dealing with Gaussian nonlinear estimation problems [8]. To construct the basic models in the interacting model algorithm, two filters are formulated. In the first model, quaternion-based extended Kalman filter (QBKF) processes quaternions transformed from signals of gyroscope, accelerometer and magnetometer; while in the second model, gyroscope-based extended Kalman filter (GBKF) processes the signal only from gyroscope. The structure of a quaternion-based extended Kalman filter is shown in Fig. 1. The related details of the design can be found in [2], [3].

The formulation of quaternions for the QBKF is based on the rotation computation. Measurements from accelerometer and magnetometer are transformed into quaternion, and then

combined with the rotating angle to form the state vector. The state equation is written as

$$\begin{bmatrix} \dot{x}_1 \\ \dot{x}_2 \\ \dot{x}_3 \end{bmatrix} = \frac{-1}{\tau} \begin{bmatrix} \omega_1 \\ \omega_2 \\ \omega_3 \end{bmatrix} \quad (11)$$

$$\begin{bmatrix} \dot{x}_4 \\ \dot{x}_5 \\ \dot{x}_6 \\ \dot{x}_7 \end{bmatrix} = \frac{1}{2} \begin{bmatrix} q_0 \\ q_1 \\ q_2 \\ q_3 \end{bmatrix} \otimes \begin{bmatrix} 0 \\ \omega_1 \\ \omega_2 \\ \omega_3 \end{bmatrix}$$

where τ is a time constant.

In using the extended Kalman filters for state estimation, estimation errors may be affected by the assumed process model and the noises in the measurements [8]. Though the measures from accelerometer can be used in supplementing the function of gyroscope, an accelerometer tends to have larger errors than other measurements, and therefore affects the performance of the QBKF. In the contrast, the sole gyroscope measures in GBKF suffer from drifting problem in time. Since the performance of both filters may degrade in different situations, it is hoped that the interacting multiple model algorithm may adapt to the signal status and characteristics, and provide estimates with minimum errors.

B. The Interacting Multiple Model (IMM) Algorithm

The IMM algorithm uses Markov chain state probabilities to weight the input and output of a bank of parallel extended Kalman filters at each time instant [5]. The estimates in our case are obtained by combining the estimates from the QBKF and GBKF, which run in parallel but based on different state models. The scheme of IMM-Based EKF is shown in Fig. 2, and the IMM algorithm is summarized as follows.

1) Calculation of mixing probabilities:

$$\mu_k(i|j) = \frac{1}{\bar{c}_j} p_{ij} \mu_k(i) \quad (12)$$

where \bar{c}_j is a normalizing constant, obtained as

$$\bar{c}_j = \sum_{i=1}^n p_{ij} \mu_k(i) \quad (13)$$

The p_{ij} is the known mode transition probabilities and the μ_k is the model probability.

2) Mixing:

$$\hat{\mathbf{X}}_{k|k}^{(oj)} = \sum_{i=1}^n \hat{\mathbf{X}}_{k|k}^{(i)} \mu_k(i|j) \quad (14)$$

$$\hat{\mathbf{P}}_{k|k}^{(oj)} = \sum_{i=1}^n \mu_k(i|j) (\mathbf{P}_{k|k}^{(j)} + (\hat{\mathbf{X}}_{k|k}^{(i)} - \hat{\mathbf{X}}_{k|k}^{(j)}) (\hat{\mathbf{X}}_{k|k}^{(i)} - \hat{\mathbf{X}}_{k|k}^{(j)})^T) \quad (15)$$

3) Model-matched filtering:

The state estimate $\hat{\mathbf{X}}_{k+1|k+1}^{(j)}$ and its covariance $\hat{\mathbf{P}}_{k+1|k+1}^{(j)}$ conditioned on each EKF model are evaluated. The likelihood function for the given model is

$$\Lambda_{k+1}^{(j)} = \frac{\exp(-(d_{k+1}^{(j)})^2/2)}{\sqrt{(2\pi)^M |\mathbf{S}_{k+1}^{(j)}|}} \quad (16)$$

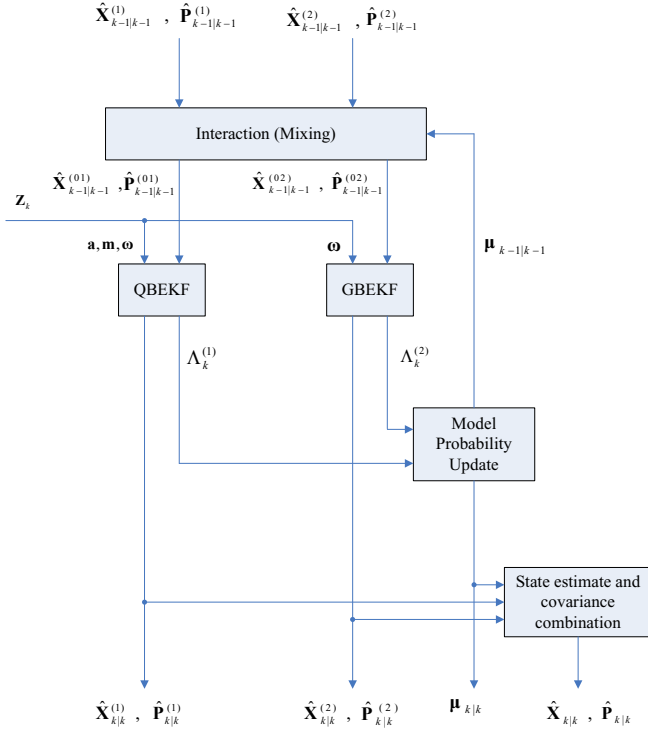


Fig. 2. The block diagram of the IMM-based estimator.

where

$$(d_{k+1}^{(j)})^2 = \mathbf{v}_{k+1}^{(j)} (\mathbf{S}_{k+1}^{(j)})^{-1} (\mathbf{v}_{k+1}^{(j)})^T \quad (17)$$

and $\mathbf{v}_k^{(j)} + 1$ is the innovation vector and $\mathbf{S}_{k+1}^{(j)}$ is a variance matrix.

4) Model probability update:

Using Bayes's rule, the updated model probability becomes

$$\mu_{k+1}^{(j)} = \frac{\Lambda_{k+1}^{(j)} \bar{c}_j}{\sum_{j=1}^n \Lambda_{k+1}^{(j)} \bar{c}_j} \quad (18)$$

5) Estimate and covariance combination:

$$\hat{\mathbf{X}}_{k+1|k+1} = \sum_{j=1}^n \hat{\mathbf{X}}_{k+1|k+1}^{(j)} \mu_{k+1}^{(j)} \quad (19)$$

$$\hat{\mathbf{P}}_{k+1|k+1} = \sum_{j=1}^n \mu_{k+1}^{(j)} \{ \mathbf{P}_{k+1|k+1}^{(j)} + \hat{\mathbf{Y}}_{k+1|k+1}^{(j)} \} \quad (20)$$

where

$$\hat{\mathbf{Y}}_{k+1|k+1}^{(j)} = (\hat{\mathbf{X}}_{k+1|k+1}^{(j)} - \hat{\mathbf{X}}_{k+1|k+1})(\hat{\mathbf{X}}_{k+1|k+1}^{(j)} - \hat{\mathbf{X}}_{k+1|k+1})^T \quad (21)$$

By using the IMM algorithm, the results of QBEKF and GBEKF are weighted and fused. A model with less error at a time instant is weighted more than the other one, and therefore, the overall estimation error can be minimized.

IV. SIMULATION RESULTS

To verify the performance of the proposed scheme, we use MATLAB to implement the IMM-Based EKFs.

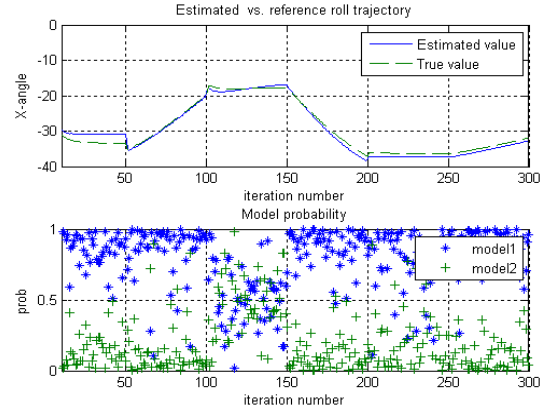


Fig. 3. Model probabilities under high gyroscope errors.

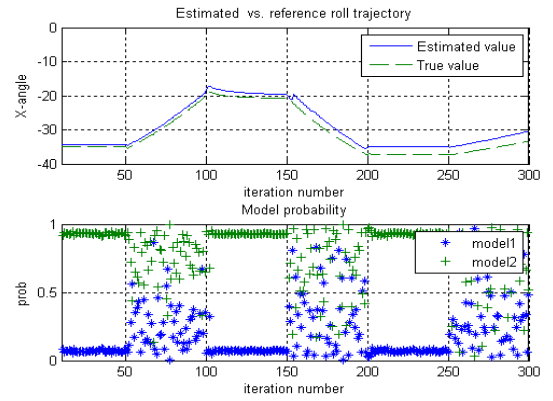


Fig. 4. Model probabilities under high accelerometer error.

A. Estimated Orientation

Assume that static measurements are observed in the Y and Z axes. Let $\sigma_M = 0.001(mGauss)$, $\sigma_A = 0.001(m/s^2)$, $\sigma_G = 0.1(m/s^2)$ and the bias of gyroscope is set to $0.0001(rad/s)$. A high variance of the measurement noise in the gyroscope is observed. It can be seen in Fig. 3 that the IMM algorithm will integrate the measurements with higher weights for model1. The model probability for QBEKF is higher than that of GBEKF. In another example, let $\sigma_M = 0.001(mGauss)$, $\sigma_A = 0.1(m/s^2)$, $\sigma_G = 0.001(m/s^2)$, and $\omega_{bias} = 0.0001(rad/s)$. A high variance of the measurement noise in the accelerometer is observed. In the simulation results, the QBEKF and GBEKF are used as model1 and model2, respectively. It can be seen in Fig. 4 that the IMM algorithm integrates the measurements with higher weights for model2. The model probability for GBEKF is higher than that of QBEKF.

To further investigate the functions of the IMM-based extended Kalman filters, the motion of a moving target is measured. For simplicity, assuming that the status in both Y-axis and Z-axis are static, only the roll angle along the X-axis varies with time. Let $\sigma_M = 0.001(mGauss)$, $\sigma_A = 0.01(m/s^2)$, $\sigma_G = 0.01(rad/s)$ and $\omega_{bias} = 0.001(rad/s)$.

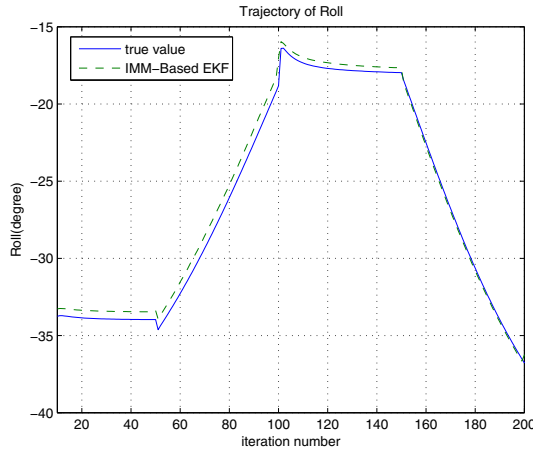


Fig. 5. Trajectory of roll with respect to X-axis

The true and estimated trajectories of roll in the X -axis are illustrated in Fig. 5. It is seen that though minor tracking errors exist, the tracking filters generally perform as expected. In Fig. 5, rapid roll angle changes are observed from samples 50 to 100. Without the measures from accelerometer and magnetometer, large errors on the estimates of GBEKF are obtained, as shown in Fig. 6. Once the rapid roll angle change no longer exists (near sample 100), the GBEKF responds quickly, and the MSE reduces to a lower level. In the contrast, the MSE of QBEKF maintains a lower level until sample 100, when the motion status changes from rotary to static. Since the accelerometer is not as sensitive as the gyroscope in responding to abrupt changes from motion to static status, the MSE raises to a high level before the adjustment in QBEKF takes effects, and thereafter the MSE starts to drop to the low level.

To deal with the different levels of MSEs from the models, the IMM-based scheme successfully integrates the estimates with associated model probabilities. When a model generates higher level of errors, lower model probability will be assigned accordingly. The transitions of model probabilities for the two models are shown in Fig. 7.

V. CONCLUSIONS

We propose an IMM-based extended Kalman filtering scheme for real-time three-dimensional motion estimation and tracking. Two models, gyroscope-based GBEKF and quaternion-based QBEKF are formulated in the interacting algorithm for data integration. Preliminary results from simulations show that, with the fusion capability in the IMM algorithm, the proposed scheme accordingly reduces the errors caused by accelerometer and gyroscope, and effectively provides better tracking results than those obtained from stand-alone models.

REFERENCES

[1] K. Maenaka, "MEMS inertial sensors and their applications," in *5th International Conference on Networked Sensing Systems*, 2008, pp. 71–73.

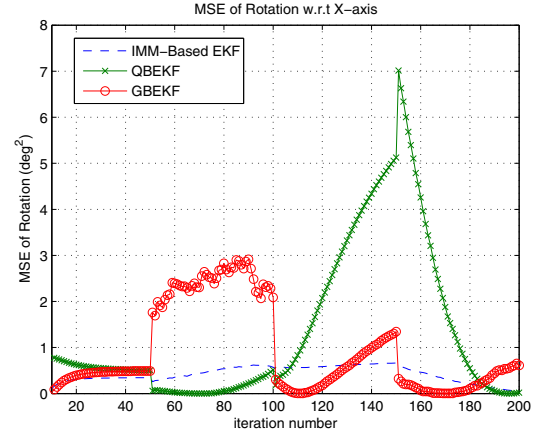


Fig. 6. Comparison of Mean square errors

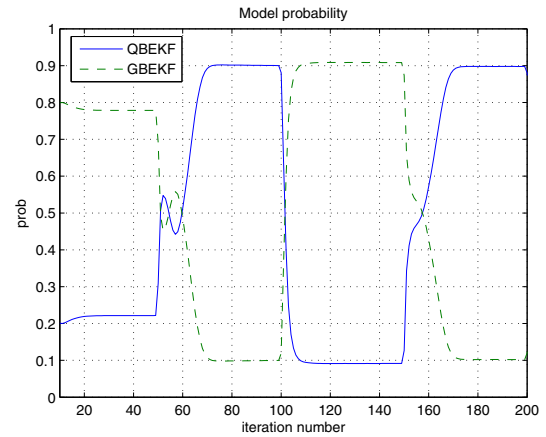


Fig. 7. Model probabilities of QBEKF and GBEKF in IMM

[2] X. Yun and E. R. Bachmann, "Design, implementation, and experimental results of a quaternion-based Kalman filter for human body motion tracking," *IEEE Transactions on Robotics*, vol. 22, no. 6, pp. 1216–1227, 2006.

[3] X. Yun, M. Lizarraga, E. Bachmann, and R. McGhee, "An improved quaternion-based Kalman filter for real-time tracking of rigid body orientation," in *IEEE/RSJ International Conference on Intelligent Robots and Systems*, vol. 2, 2003, pp. 1074–1079.

[4] J. Chou, "Quaternion kinematic and dynamic differential equations," *IEEE Transactions on Robotics and Automation*, vol. 8, no. 1, pp. 53–64, 1992.

[5] Y. Bar-Shalom, K. Chang, and H. Blom, "Tracking a maneuvering target using input estimation versus the interacting multiple model algorithm," *IEEE Transactions on Aerospace and Electronic Systems*, vol. 25, no. 2, pp. 296–300, 1989.

[6] D.-J. Jwo and C.-H. Tseng, "GPS navigation processing using the IMM-based EKF," in *Sensing Technology, 2008. ICST 2008. 3rd International Conference on*, 2008, pp. 589–594.

[7] J. Marins, X. Yun, E. Bachmann, R. McGhee, and M. Zyda, "An extended Kalman filter for quaternion-based orientation estimation using MARG sensors," in *IEEE/RSJ International Conference on Intelligent Robots and Systems*, vol. 4, 2001, pp. 2003–2011.

[8] S. M. Kay, *Fundamentals of statistical signal processing: Estimation Theory*. New Jersey: Prentice Hall, 1993, vol. 1.